DOI: 10.1007/s11099-014-0046-5 PHOTOSYNTHETICA 52 (3): 413-420, 2014

Photosynthetic electron flow during leaf senescence: Evidence for a preferential maintenance of photosystem I activity and increased cyclic electron flow

C. KOTAKIS[*, **, +], A. KYZERIDOU[*], and Y. MANETAS[*]

Laboratory of Plant Physiology, Department of Biology, University of Patras, Patras GR-26500, Greece[*]
Institute of Plant Biology, Biological Research Center, Hungarian Academy of Sciences, P.O. Box 521, H-6701 Szeged, Hungary[**]

Abstract

Limitations in photosystem function and photosynthetic electron flow were investigated during leaf senescence in two field-grown plants, *i.e., Euphorbia dendroides* L. and *Morus alba* L., a summer- and winter-deciduous, shrub and tree, respectively. Analysis of fast chlorophyll (Chl) *a* fluorescence transients and post-illumination fluorescence yield increase were used to assess photosynthetic properties at various stages of senescence, the latter judged from the extent of Chl loss. In both plants, the yield of primary photochemistry of PSII and the content of PSI remained quite stable up to the last stages of senescence, when leaves were almost yellow. However, the potential for linear electron flow along PSII was limited much earlier, especially in *E. dendroides,* by an apparent inactivation of the oxygen-evolving complex and a lower efficiency of electron transfer to intermediate carriers. On the contrary, the corresponding efficiency of electron transfer from intermediate carriers to final acceptors of PSI was increased. In addition, cyclic electron flow around PSI was accelerated with the progress of senescence in *E. dendroides*, while a corresponding trend in *M. alba* was not statistically significant. However, there was no decrease in PSI activity even at the last stages of senescence. We argue that a switch to cyclic electron flow around PSI during leaf senescence may have the dual role of replenishing the ATP and maintaining a satisfactory nonphotochemical energy quenching, since both are limited by hindered linear electron transfer.

Additional key words: alternative routes; electron flow; chlorophyll fluorescence; chloroplast; photosynthesis; senescence regulation.

Introduction

Leaf senescence is a complicated and highly regulated process which is optically manifested as a loss of greenness. At the biochemical level, Chl is dissociated from the chloroplast membranes and enzymatically decomposed to colourless products, so that possible photodynamic production of reactive oxygen species is prevented (Ougham *et al*. 2005). Concurrently, thylakoids are dismantled and both membrane and stromal proteins (including Rubisco) are degraded, while the resulting nutrients, especially nitrogen, are remobilized to permanent organs to be reused during the following growth season (Matile 2000, Hörtensteiner 2004). Apparently, the execution of the senescence program requires the induction of specific genes coding for catabolic enzymes, while the expression of anabolic genes is downregulated (Buchanan-Wollaston *et al*. 2003). As a result, the CO_2 assimilation capacity of a senescing leaf is gradually lost (Keskitalo *et al*. 2005) and the linear electron transport rate through PSII reaction center complex is diminished (Lu *et al*. 2003) However, the maximum photochemical efficiency of the remaining PSII centers remains high up to later stages of chloroplast deterioration (Adams *et al*. 1990, Lu *et al*. 2003, Manetas and Buschmann 2011). One may argue that the parallel fall in CO_2 assimilation and linear electron transport rates may reflect the weakening of the carbon reduction cycle to act as a sink of ATP and electrons, and the concomitant need

Received 14 January 2014, *accepted* 7 April 2014.
[+]Corresponding author: kotakisx@yahoo.gr
Abbreviations: Chl – chlorophyll; F_0 – minimal fluorescence yield; F_J or F_I − fluorescence intensity at 2 ms or 30 ms, respectively; F_m – maximal fluorescence yield; F_v – maximal variable fluorescence; OEC – oxygen-evolving complex; RC – reaction centers; RE − reduction of end electron acceptors; V_I − relative variable fluorescence at 30 ms; V_J − relative variable fluorescence at 2 ms; V_K − relative variable fluorescence at 300 μs; δ_{R0} − the efficiency of electron transfer between intermediate carriers to the RE of PSI; φ_{P0} – maximal quantum yield of PSII primary photochemistry, taken as equal to F_v/F_m; ψ_{E0} − the efficiency of trapped energy to move an electron further than Q_A^-. All the above fluorescence parameters refer to dark-adapted state.

for a downregulation of linear electron flow. However, the specific limiting steps in electron flow from H_2O to the final electron acceptors of PSI have not been investigated in senescing leaves.

Such an investigation could be attained by analyzing the kinetics of the polyphasic (O-J-I-P) fast Chl *a* fluorescence transients upon sudden illumination of dark-adapted leaves. The fluorescence induction curve, if plotted on a logarithmic time scale, displays the intermediate steps of the sequential fluorescence increase, reflecting a corresponding stepwise flow of energy and the gradual reduction of electron flow components (Strasser *et al*. 2004, Tsimilli-Michael and Strasser 2008, Stirbet and Govindjee 2011). For example, an increase in the relative fluorescence at 300 μs (K-step) indicates a possible limitation due to inactivation of the oxygen-evolving complex (OEC, Srivastava *et al*. 1997), and/or due to a different functional antenna size (Yusuf *et al.* 2010). Limitations in the efficiency of electron flow from PSII to intermediate carriers are expressed as changes in the relative fluorescence at the J-step (2 ms) (Tsimilli-Michael and Strasser 2008, Jiang *et al*. 2008). Finally, the upper part of the Chl fluorescence transient, *i.e*., the I-P phase from 30 ms to the peak fluorescence, is affected by changes in the efficiency of electron flow from intermediate carriers to the end electron acceptors of PSI and by the PSI content (Schansker *et al*. 2005, Oukarroum *et al*. 2009, Ceppi *et al*. 2012). Hence, the complete analysis of O-J-I-P curves allows a detailed assessment of structural and functional adjustments along the whole continuum of energy and electron flow from initial donors of PSII to the final acceptors of PSI.

In the present paper, we applied this analysis to investigate the sequence of events and the development of specific limitations in light reactions during the transformation of chloroplasts to gerontoplasts. To that aim, naturally senescing leaves from two woody species, one summer- and one winter-deciduous, were used. Since in both cases PSI content was not affected even at the final stages of senescence, the potential for cyclic electron flow was also examined.

Materials and methods

Plants and sampling: *E. dendroides* (L.) is a Mediterranean shrub (rarely tree) occupying the dry end of precipitation gradient and responding to summer drought by shedding its foliage. A population near Galaxidi (38.35°N, 22.37°E, 67 m a.s.l.) was used in this study. *M. alba* (L.) is a winter, deciduous, temperate tree. A specimen grown as ornamental in the Patras University campus (38.29°N, 21.79°E, 63 m a.s.l.) was used. In both plants, leaf senescence is not synchronous and at a given sampling date one may find the whole range of leaf colours from full green to full yellow. Sampling was performed at late afternoon during consecutive days during May 2011 for *E. dendroides* and in November 2012 for *M. alba*. Only south-facing, fully exposed leaves were harvested to avoid confounding effect of shading. The cut leaves were enclosed in small, air-tight, plastic bags lined internally with moist filter paper and kept in the dark at room temperature for 12 h before analysis. During next morning, the predarkened leaves were inserted into leaf clips for Chl fluorescence measurements. Subsequently, a fiber optic was directly attached on the measured leaf spots to assess Chl content through spectral reflectance measurements.

Chl fluorescence: Fast Chl fluorescence transients of intact, dark-adapted samples were captured by a *Hansatech* fluorimeter (*Handy-PEA*, *Hansatech Instruments Ltd*., Kings' Lynn, Norfolk, UK). For excitation, a bank of three red (peak at 650 nm) LEDs provided 3,000 μmol(photon) m^{-2} s^{-1} at sample level and fluorescence was recorded from 10 μs to 1 s with data acquisition rates 10^5, 10^4, 10^3, 10^2, and 10 readings per s in the time intervals of 10–300 μs, 0.3–3 ms, 3–30 ms, 30–300 ms, and 0.3–1 s, respectively. Cardinal points in the fluorescence *vs.* time curve used for further calculation of biophysical parameters were the following: maximal recorded fluorescence intensity (F_P), taken as equal to F_m (the fluorescence intensity when all RCs are closed), since the strong actinic illumination applied ensures the closure of all RCs; the first credible measured fluorescence intensity (at 20 μs, $F_{20\mu s}$), taken as (about) equal to F_0 (the fluorescence intensity when all RCs are open); fluorescence intensity at 300 μs ($F_{300\mu s}$), needed for the calculation of V_K; fluorescence intensity at 2 and 30 ms, *i.e.*, at the J and I steps, respectively (F_J and F_I). These primary data were used to derive the following parameters according to the JIP-test (Strasser *et al*. 2004), as extended to analyze also events in or around PSI (Jiang *et al*. 2008, Tsimilli-Michael and Strasser 2008, Oukarroum *et al*. 2009).

The photosynthetic efficiencies at the onset of illumination, *i.e.*, the maximum quantum yield of primary photochemistry $\varphi_{P0} = TR_0/ABS = (F_m - F_0)/F_m = F_v/F_m$ (where TR and ABS denote the trapped and absorbed excitation energy fluxes); the efficiency of trapped energy to move an electron further than Q_A^- (*i.e.*, electron transfer, ET) $\psi_{E0} = ET_0/TR_0$; the efficiency of electron transfer between intermediate carriers to the reduction of end electron acceptors (RE) of PSI, $\delta_{R0} = RE_0/ET_0$.

The ratio V_K/V_J was used as a relative measure of a) inactivation of OEC (Kalachanis and Manetas 2010) and/or of b) the functional antenna size (Yusuf *et al.* 2010).

The relative amplitude of the I-P phase, $1 - V_I$, reflects the content of PSI reaction centers (Oukarroum *et al*. 2009, Ceppi *et al*. 2012) as well as the electron flow capacity from plastoquinone to the PSI electron acceptors (Schansker *et al.* 2005).

The formulae used for the calculation of the above parameters are given in the Appendix.

Cyclic electron flow: The relative magnitude of cyclic electron flow around PSI was assessed through the post-illumination transient increase in fluorescence yield after turning off actinic light (Mano *et al*. 1995, Munné-Bosch *et al*. 2005). For that purpose, dark-adapted (1 h) leaves were inserted into the leaf clip of a *MINI-PAM* fluorimeter (*Waltz*, Effeltrich, Germany) and illuminated for 4 min at 850 μmol(photon) m^{-2} s^{-1} by an external white light source. Upon light/dark transition, the fluorescence yield dropped suddenly to a value approaching F_0 (hereby defined as F_0') and subsequently displayed a transient increase to a peak value (hereby defined as F_0^P) within the next 60 s. This increase is due to dark reduction of plastoquinone by stromal reductants and it is considered as a measure of the potential for cyclic electron flow. It is quantified by the parameter $(F_0^P - F_0')/F_0^P$ (Kotakis *et al*. 2006).

Chl content: Spectral reflectance was measured with a spectroradiometer (*Unispec*, *PPSystems*, Haverhill, USA) equipped with an internal white light source and a bifurcated optical fiber directly and perpendicularly attached on the leaf. A spectralon standard (95% reflectance along the whole 400−1,100 nm effective spectral band) was used to calibrate the instrument. Chl concentration was estimated by using the spectral index and formula given by Gitelson *et al*. (2009). Accordingly, Chl [nmol cm^{-2}] = (CI − 0.0319)/0.0737, where CI (Chl index) = $(R_{NIR}/R_{red\ edge}) - 1$ and R_{NIR} and $R_{red\ edge}$ are the mean reflectances at 770–800 and 690–710 nm, respectively.

Statistics: Best fit lines and levels of significance were computed with the *SPSS 9.0* statistical package. Each curve in Figs. 2−6 represents the values of 122 independent measurements for *E. dendroides* and 32 independent measurements for *M. alba*. In case of cyclic electron flow, the curves represent the values of 34 and 24 independent measurements for *E. dendroides* and *M. alba*, respectively.

Results

Chl fluorescence rise curves obtained from the dark-adapted leaves of both plants and expressed on a logarithmic time scale showed typical O-J-I-P transients (Fig. 1*A*,*B*), irrespective of the senescence state. However, a closer comparison between samples of varying Chl content revealed considerable kinetic differences. In Fig. 1*C*,*D*, the transients of a fully green and a partly senescent leaf were given as relative variable fluorescence (V_t, *i.e.*, double normalized at the F_0 and F_P points). The differences were maximized at the low and medium part of the curves, especially around the K-band (300–600 μs) and the J-step (2 ms). This was better shown in Fig. 1*E*,*F*, as ΔV_t, *i.e.*, the arithmetic difference between the kinetics of a senescent minus a green leaf. On the contrary, the differences at the high part of the curve were minimized. Altogether, this initial qualitative approach indicated that during senescence both the oxidizing and reducing sides of PSII were affected more than PSI. The above was confirmed by detailed numerical analysis of the O-J-I-P transient at various stages of leaf senescence as shown below.

The maximum PSII photochemical efficiency, φ_{P0} (equivalent to F_v/F_m) remained high in both plants even at the advanced stages of leaf senescence, when more than 70% and 85% of Chl was degraded in *E. dendroides* and *M. alba*, respectively (Fig. 2). Thereafter, it declined considerably. However, the parameter ψ_{E0} started to decrease much earlier, especially in *E. dendroides* (Fig. 3*A*), indicating a limitation in the energy trapped in PSII to be conserved as electron flow to intermediate carriers. Although dark reduction of plastoquinone is possible, it is known that such fluxes proceed at an exceedingly low rate (Groom *et al.* 1993, Feild *et al.* 1998) and hence, the possible partial reduced plastoquinone pool can not affect significantly the level of the J-level of the fluorescence induction measurements. Moreover, the parameter V_K/V_J was gradually increasing, indicating an additional limitation probably linked with the OEC (Fig. 4) and/or due to a different functional antenna size (Yusuf *et al.* 2010). Again, the senescence-induced increase in V_K/V_J was earlier and more pronounced in *E. dendroides* (compare Fig. 4*A* with 4*B*).

The two parameters related to PSI, *i.e.*, δ_{R0} indicating the efficiency of electron flow from intermediate carriers to the final PSI acceptors, and the amplitude of the I-P phase ($1 - V_I$), indicating the content of PSI and the ability for plastoquinone reoxidation by PSI activity (Schansker *et al.* 2005, Ceppi *et al.* 2012), behaved in a different manner. δ_{R0} was continuously increasing during senescence in *E. dendroides* (Fig. 5*A*), but it was constant in *M. alba* up to a Chl loss of *ca*. 80%, to be increased thereafter (Fig. 5*B*). The PSI capacity ($1 - V_I$) was very slightly decreasing in *E. dendroides* (Fig. 6*A*), while in *M. alba* it remained constant until Chl reached 80% of its initial value.

We argued that the apparent limitation in electron flow through PSII, in conjunction with the absence of such limitation through PSI and the relative stability of PSI content, might predispose to an increased cyclic electron flow around PSI in senescing leaves. Hence, in separate experiments, we examined the possible correlation between cyclic electron flow and Chl content. As shown in Fig. 7*A*, cyclic flow in *E. dendroides* increased considerably with Chl degradation, while despite seeing a similar trend it was not statistically significant in *M. alba* (Fig. 7*B*). However, importantly, cyclic electron flow continued at appreciable rates even during the last stages of leaf senescence in both species.

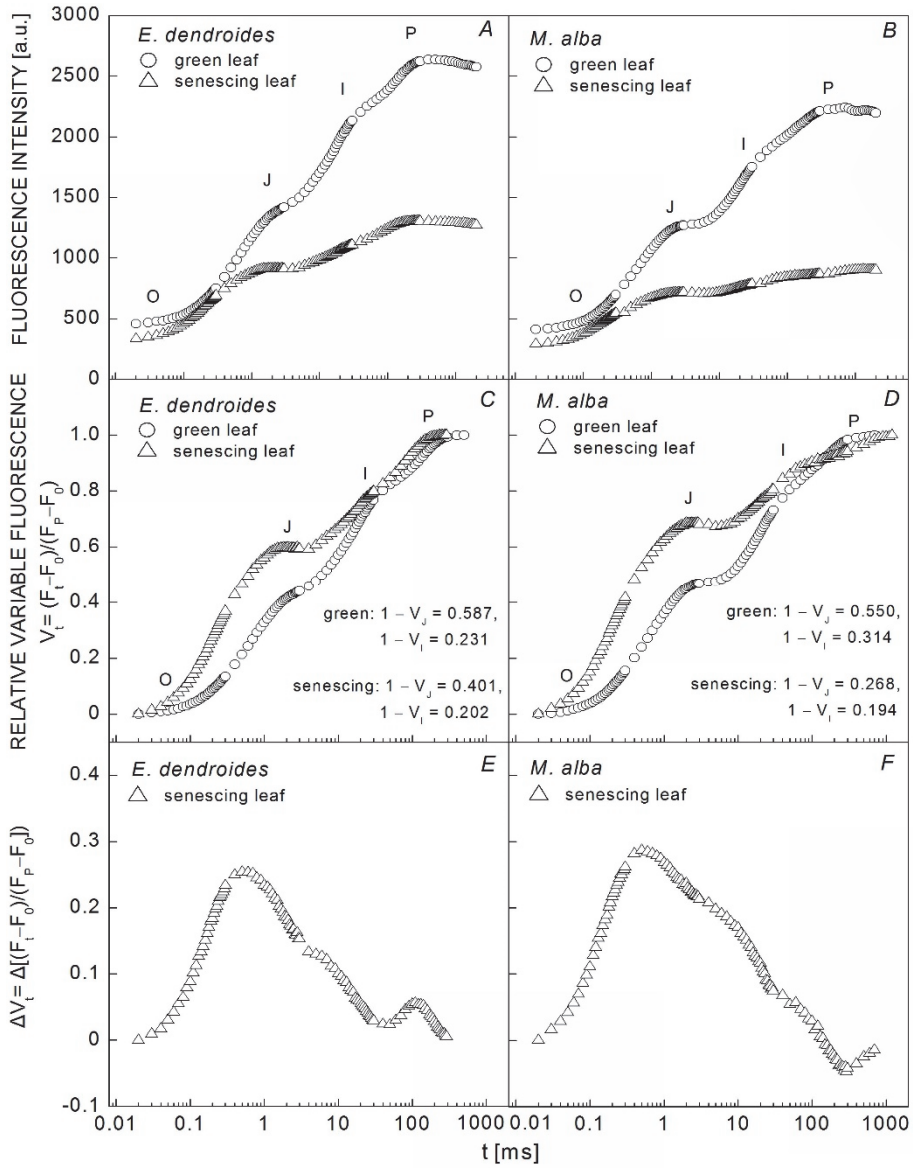

Fig. 1. Raw fluorescence data from a green (*circles*) and a senescing (*triangles*) leaf of *E. dendroides* (*A*) and *M. alba* (*B*) given on a logarithmic time scale. Representative fast chlorophyll fluorescence transients (O-J-I-P) based on the data of Fig.1*A*,*B* for the indicated species (*C*,*D*) given on a logarithmic time scale and expressed as relative variable fluorescence (V_t), *i.e.*, double normalized at the F_0 and F_P points. The fluorescence intensity at P is considered as equal to the F_m (the fluorescence intensity when all RCs are closed), due to the strong illumination used for fluorescence induction. Corresponding chlorophyll concentrations at 51 and 6 nmol cm^{-2}, respectively. Differences in fast chlorophyll fluorescence transients between green and senescing leaves (*E*,*F*). Values obtained from the data of Fig.1*C*,*D* by subtracting the green leaf transient from the senescing leaf transient.

Discussion

It is evident from the results of this investigation that maximum PSII photochemical efficiency was affected only at the very last stages of Chl degradation (Fig. 2). Hence, in spite of the considerable breakdown of LHC and Rubisco (Hörtensteiner and Feller 2002), the PSII photon trapping efficiency remained intact and senescing leaves did not suffer from appreciable photoinhibition. This is in accordance to previous results of various papers (Adams *et al*. 1990, Miersch *et al*. 2000, Lu *et al*. 2003, Manetas and Buschmann 2011). However, severe limitations were observed in the electron flow both at the reducing and oxidizing sides of PSII, as shown by the low probability for trapped excitons to induce electron flow to intermediate carriers (ψ_{E0}, Fig. 3) and the partial inactivation of the OEC (V_K/V_J, Fig. 4). Hence, a decrease in linear electron flow along PSII might be expected. Indeed, this

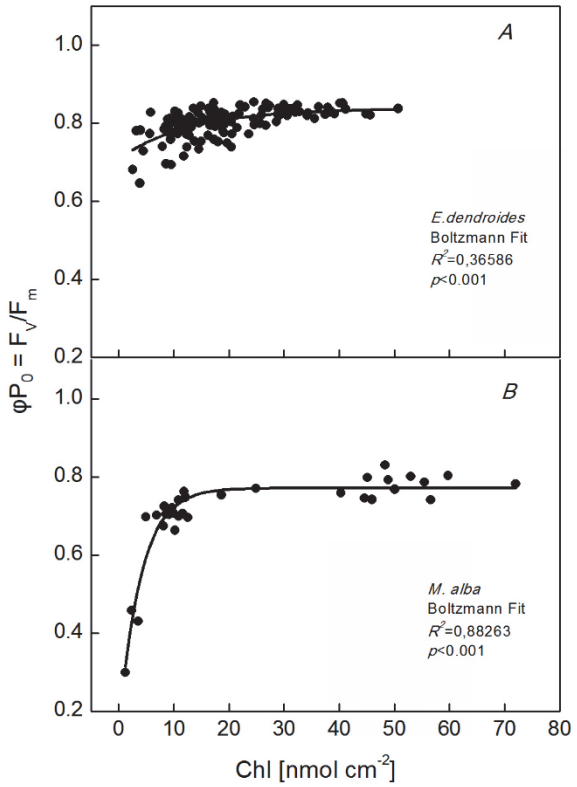

Fig. 2. Maximum PSII photochemical efficiency ($\varphi_{P0} = F_v/F_m$) *vs*. leaf chlorophyll (Chl) concentration during leaf senescence.

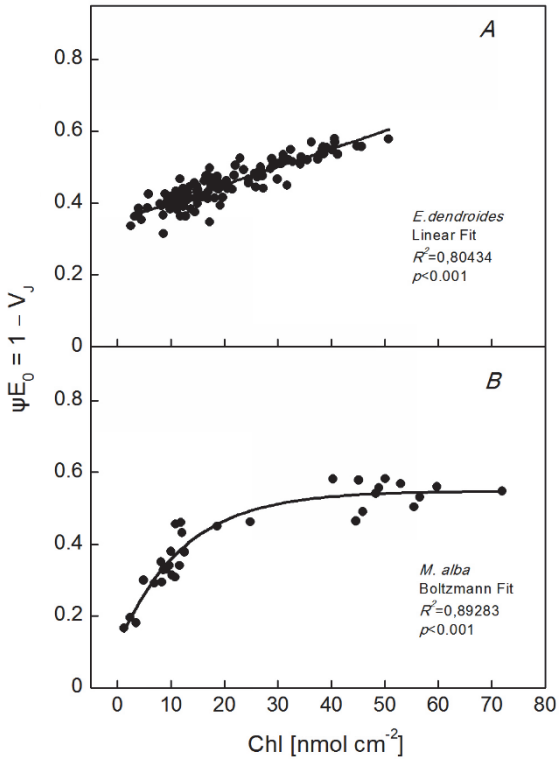

Fig. 3. Efficiency of trapped energy conservation as electron transfer to intermediate carriers ($\psi_{E0} = 1 - V_J$) *vs*. chlorophyll (Chl) concentration during leaf senescence.

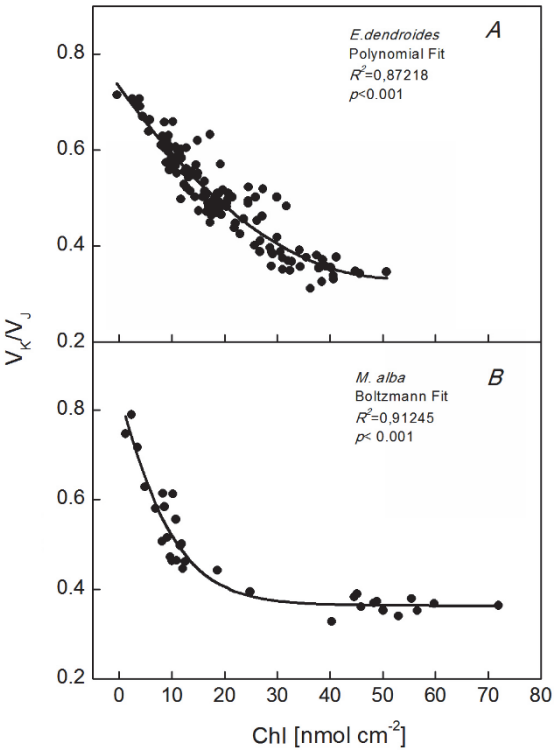

Fig. 4. Relative inactivation of the oxygen-evolving complex and/or increment of the functional antenna size (as V_K/V_J) *vs*. chlorophyll (Chl) concentration during leaf senescence.

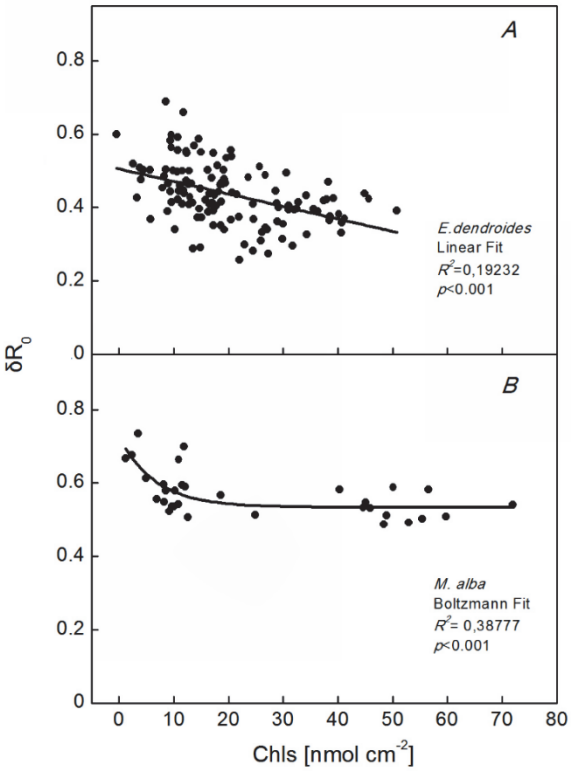

Fig. 5. Efficiency of electron flow from intermediate electron carriers to final acceptors of PSI (δ_{R0}) *vs*. chlorophyll (Chl) concentration during leaf senescence.

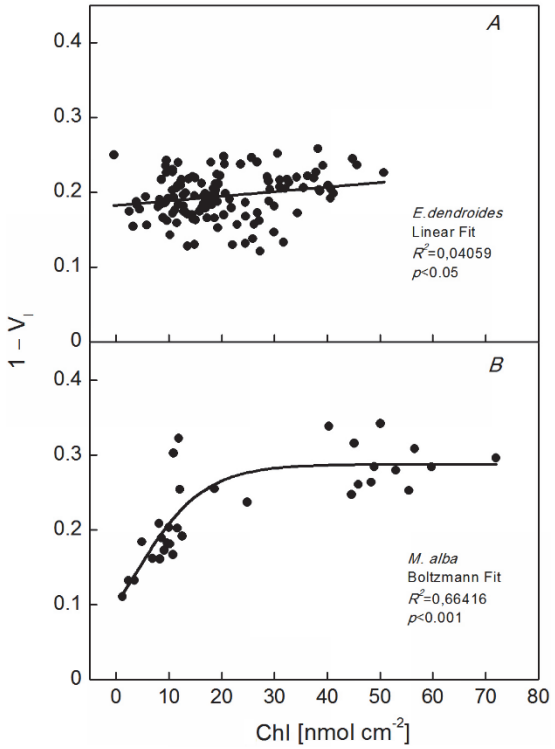

Fig. 6. Relative content of PSI reaction centers (as $1 - V_I$) *vs*. chlorophyll (Chl) concentration during leaf senescence.

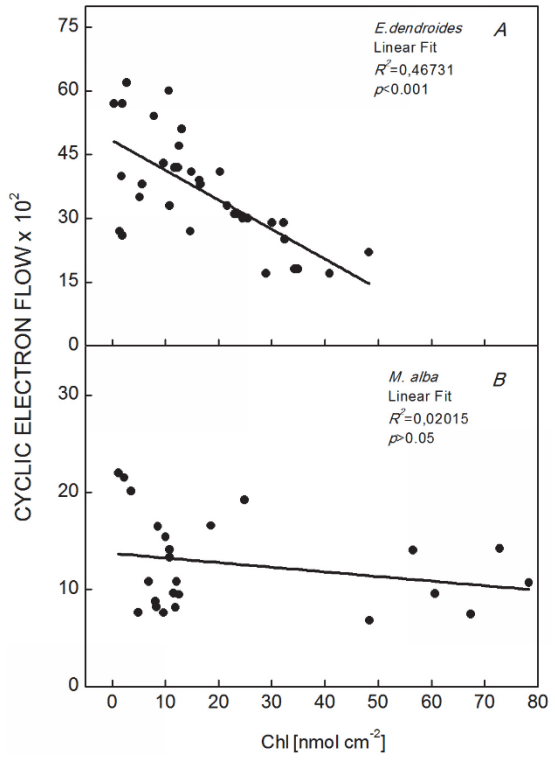

Fig. 7. Cyclic electron flow around PSI (as $(F_0^P - F_0')/F_0^P$) *vs*. chlorophyll (Chl) concentration during leaf senescence. Scales of vertical axis are different between the indicated species.

has been shown in light-adapted senescing leaves (Lu *et al*. 2003). Moreover, the increase of the V_K/V_J ratio during senescence found in our study can as well be interpreted as an increase of the functional antenna size, which might mean that PSII reaction centers were degraded before their LHCII and the reaction centers-less LHCII was supplying excitation energy to the remaining reaction centers.

Up to this point, our results simply confirmed previous studies. However, limitations in the function of PSI were less obvious and, contrary to expectations for a degrading chloroplast, electron flow through this photosystem seemed to be facilitated. The parameter $\delta_{R0} = (1 - V_I)/(1 - V_J)$, steadily increased with Chl loss in *E. dendroides* (Fig. 5*A*), because $(1 - V_I)$ remained practically constant (Fig. 6*A*) and only $(1 - V_J)$ decreased, upon Chl degradation. While δ_{R0} remained constant with the progress of senescence in *M. alba*, because both $(1 - V_I)$ and $(1 - V_J)$ decreased in the same way, and it increased considerably at the last stages (Fig. 5*B*). Hence, once an electron from PSII manages to reduce an intermediate carrier, the probability of its further flow through PSI is increased with the progress of senescence. Moreover, the almost constant levels of PSI during senescence (Fig. 6) may not hinder such a flow.

The apparent facilitation of electron flow from intermediate electron carriers to final acceptors of PSI seems futile, since the electron sink capacities of both CO_2 assimilation and photorespiration cycles in senescing leaves are severely diminished due to extensive Rubisco degradation (Hörtensteiner and Feller 2002). Hence, we argued that alternative electron transfer pathways might be activated. Indeed, cyclic electron flow through PSI increased considerably, at least in *E. dendroides* (Fig. 7). In the case of *M. alba*, other alternative electron routes could also be possible such as chlororespiration (Rumeau *et al.* 2007) since (*1*) the corresponding cyclic electron flow trend was not statistically significant (Fig. 7) with the PSI activity remaining almost constant, taken together with (*2*) a more pronounced inhibition of the linear electron flow (Figs. 2,3,6) in comparison to *E. dendroides*.

Cyclic electron transfer around PSI results in plastoquinone reduction at the expense of stromal electron donors, mainly NADPH and ferredoxin. It is mediated by either NAD(P)H dehydrogenase (NDH) or ferredoxin-plastoquinone reductase (FQR) (Bukhov and Carpentier 2004, Rumeau *et al*. 2007). The expression of these enzymes as well as the activity of the cyclic pathway are enhanced during heat, drought, and high light plus low-temperature stresses (*see* reviews cited above). Hence, cyclic electron flow may be linked to stress adaptation (Niyogi 2000). It may not be irrelevant that expression of corresponding genes and activity of NDH are also induced during senescence (Martín *et al*. 1996), indicating a possible role of plastid genes in programmed cell death (Zapata *et al*. 2005).

Under normal conditions, cyclic electron flow around

PSI is particularly useful in bundle sheath cells of C_4 plants (Edwards and Walker 1983). Since chloroplasts in these cells are deficient in PSII and, accordingly, in ATP produced through linear electron flow, PSI-driven cyclic electron transfer is believed to supply the ATP required for CO_2 fixation. Similarly, an engagement of cyclic electron flow was shown in green petioles and twigs, where a part of the photosynthetically fixed CO_2 derives from decarboxylation of C_4 organic acids in the ascending transpiration stream (Ivanov *et al*. 2006, Kotakis *et al*. 2006, Brown *et al*. 2010). Depending on the nature of the decarboxylated material, either extra ATP is consumed or extra NADPH is produced (Edwards and Walker 1983). Hence, cyclic electron flow in these cases may adjust the required ATP/NADPH ratio. In these green, nonphotosynthetic organs, linear electron flow is considerably impaired (Hetherington *et al*. 1998, Manetas 2004).

On the basis of the above, we may ascribe a functional role for cyclic electron flow in providing the necessary ATP for the execution of the senescence program and the remobilization of nutrients. Based on the degradation of chloroplasts, while mitochondria were still active even at more advanced stages of leaf senescence, Keskitalo *et al*. (2005) proposed that the energetic requirements are finally undertaken by respiration. The results of the present study suggest that local ATP needs in the degrading chloroplast, with its inhibited linear electron flow, might be still met by enhanced alternative electron routes around PSI.

Apart from adjusting the ATP/NADPH ratio, cyclic electron flow is thought to participate in the development of nonphotochemical energy quenching (Niyogi 2000) and protection against photooxidative stress (Martín *et al*. 2004) in case the absorbed photon energy exceeds that needed for CO_2 assimilation. This may be the case in senescing leaves, where Rubisco is rapidly degraded, while leaf absorptance decreases at a much slower rate than Chl concentration (Dima *et al*. 2006) and nonphotochemical quenching increases (Lu *et al*. 2003). As a result, photoinhibition of PSII (Fig. 2) and PSI (Fig. 5) was avoided.

In conclusion, this study indicates that an increase of cyclic electron flow might be significant for the smooth operation of the leaf senescence program.

References

Adams, W.W., Winter, K., Schreiber, U. *et al*.: Photosynthesis and chlorophyll fluorescence characteristics in relationship to changes in pigment and element composition of leaves of *Platanus occidentalis* L. during autumnal leaf senescence. − Plant Physiol. **92**: 1184-1190, 1990.

Brown, N.J., Palmer, B.G., Stanley, S. *et al*.: C_4 acid decarboxylases required for C_4 photosynthesis are active in the mid-vein of the C_3 species *Arabidopsis thaliana*, and are important in sugar and amino acid metabolism. − Plant J. **61**: 122-133, 2010.

Buchanan-Wollaston, V., Earl, S., Harrison, E. *et al*.: The molecular analysis of leaf senescence - a genomics approach. − Plant Biotechnol. J. **1**: 3-22, 2003.

Bukhov, N., Carpentier, R.: Alternative photosystem I-driven electron transport routes: mechanisms and functions. − Photosynth. Res. **82**: 17-33, 2004.

Ceppi, M.G., Oukarroum, A., Çiçek, N. *et al*.: The IP amplitude of the fluorescence rise OJIP is sensitive to changes in the photosystem I content of leaves: a study on plants exposed to magnesium and sulfate deficiencies, drought stress and salt stress. − Physiol. Plantarum **144**: 277-288, 2012.

Dima, E., Manetas, Y., Psaras, G.K.: Chlorophyll distribution pattern in inner stem tissues: evidence from epifluorescence microscopy and reflectance measurements in 20 woody species. – Trees-Struct. Funct. **20**: 515-521, 2006.

Edwards, G., Walker, D.A.: C_3, C_4: Mechanisms, and Cellular and Environmental Regulation of Photosynthesis. Pp. 97-520. Blackwell Scientific Publications, Oxford 1983.

Feild, T.S., Nedbal, L., Ort, D.R.: Nonphotochemical reduction of the plastoquinone pool in sunflower leaves originates from chlororespiration.− Plant Physiol. **116**: 1209-1218, 1998.

Gitelson, A. A., Chivkunova, O.B., Merzlyak, M.N.: Nondestructive estimation of anthocyanins and chlorophylls in anthocyanic leaves. − Am. J. Bot. **96**: 1861-1868, 2009.

Groom, Q., Kramer, D.M., Crofts, A.R., Ort, D.R.: The nonphotochemical reduction of plastoquinone in leaves. − Photosynth. Res. **36**: 205-215, 1993.

Hetherington, S.E., Smillie, R.M., Davies, W.J.: Photosynthetic activities of vegetative and fruiting tissues of tomato. − J. Exp. Bot. **49**: 1173-1181, 1998.

Hörtensteiner, S., Feller, U.: Nitrogen metabolism and remobilization during senescence. − J. Exp. Bot. **53**: 927-937, 2002.

Hörtensteiner, S.: The loss of green color during chlorophyll degradation - a prerequisite to prevent cell death? − Planta **219**: 191-194, 2004.

Ivanov, A.G., Krol, M., Sveshnikov, D. *et al*.: Characterization of the photosynthetic apparatus in cortical bark chlorenchyma of Scots pine. − Planta **223**: 1165-1177, 2006.

Jiang, H.X., Chen, L.S., Zheng, J.G. *et al*.: Aluminum-induced effects on photosystem II photochemistry in *Citrus* leaves assessed by the chlorophyll *a* fluorescence transient. − Tree Physiol. **28**: 1863-1871, 2008.

Kalachanis, D., Manetas, Y.: Analysis of fast chlorophyll fluorescence rise (O-K-J-I-P) curves in green fruits indicates electron flow limitations at the donor side of PSII and the acceptor sides of both photosystems. − Physiol. Plantarum **139**: 313-323, 2010.

Keskitalo, J., Bergquist, G., Gardeström, P. *et al*.: A cellular timetable of autumn senescence. − Plant Physiol. **139**: 1635-1648, 2005.

Kotakis, C., Petropoulou, Y., Stamatakis, K. *et al*.: Evidence for active cyclic electron flow in twig chlorenchyma in the presence of an extremely deficient linear electron transport activity. − Planta **225**: 245-253, 2006.

Lu, Q.T., Wen, X.G., Lu, C.M. *et al*.: Photoinhibition and photoprotection in senescent leaves of field-grown wheat plants. − Plant Physiol. Bioch. **41**: 749-754, 2003.

Manetas, Y.: Probing corticular photosynthesis through in vivo chlorophyll fluorescence measurements: evidence that high internal CO_2 levels suppress electron flow and increase the risk of photoinhibition. − Physiol. Plantarum **120**: 509-517, 2004.

Manetas, Y., Buschmann, C.: The interplay of anthocyanin biosynthesis and chlorophyll catabolism in senescing leaves and the question of photosystem II photoprotection. − Photosynthetica **49**: 515-522, 2011.

Mano, J., Miyake, C., Schreiber, U. *et al*.: Photoactivation of the electron flow from NADPH to plastoquinone in spinach chloroplasts. − Plant Cell Physiol. **36**: 1589-1598, 1995.

Martín, M., Casano, L.M., Sabater, B.: Identification of the product of *ndhA* gene as a thylakoid protein synthesized in response to photooxidative treatment. − Plant Cell Physiol. **37**: 293-298, 1996.

Martín, M., Casano, L.M., Zapata, J.M. *et al*.: Role of thylakoid Ndh complex and peroxidase in the protection against photo-oxidative stress: fluorescence and enzyme activities in wild-type and *ndhF*-deficient tobacco. − Physiol. Plantarum **122**: 443-452, 2004.

Matile, P.: Biochemistry of Indian summer: physiology of autumnal leaf coloration. − Exp. Gerontol. **35**: 145-158, 2000.

Miersch, I., Heise, J., Zelmer, I. *et al*.: Differential degradation of the photosynthetic apparatus during leaf senescence in barley (*Hordeum vulgare* L.). − Plant Biol. **2**: 618-623, 2000.

Munné-Bosch, S., Shikanai, T., Asada, K.: Enhanced ferredoxin-dependent cyclic electron flow around photosystem I and α-tocopherol quinone accumulation in water-stressed *ndhB*-inactivated tobacco mutants. − Planta **222**: 502-511, 2005.

Niyogi, K.K.: Safety valves for photosynthesis. − Curr. Opin. Plant Biol. **3**: 455-460, 2000.

Ougham, H.J., Morris, P., Thomas, H.: The colors of autumn leaves as symptoms of cellular recycling and defenses against environmental stresses. − Curr. Top. Dev. Biol. **66**: 135-160, 2005.

Oukarroum, A., Schansker, G., Strasser, R.J.: Drought stress effects on photosystem I content and photosystem II thermotolerance analyzed using Chl *a* fluorescence kinetics in barley varieties differing in their drought tolerance. − Physiol. Plantarum **137**: 188-199, 2009.

Rumeau, D., Peltier, G., Cournac, L.: Chlororespiration and cyclic electron flow around PSI during photosynthesis and plant stress response. − Plant Cell Environ. **30**: 1041-1051, 2007.

Schansker, G., Tóth, S.Z., Strasser, R.J.: Methylviologen and dibromothymoquinone treatments of pea leaves reveal the role of Photosystem I in the Chl *a* fluorescence rise OJIP. – BBA-Bioenergetics **1706**: 250-261, 2005.

Srivastava, A., Guissé, B., Greppin, H. *et al*.: Regulation of antenna structure and electron transport in photosystem II of *Pisum sativum* under elevated temperature probed by the fast polyphasic chlorophyll *a* fluorescence transient : OKJIP. − BBA-Bioenergetics **1320**: 95-106, 1997.

Stirbet, A., Govindjee: On the relation between the Kautsky effect (chlorophyll *a* fluorescence induction) and photosystem II: Basics and applications of the OJIP fluorescence transient. − J. Photoch. Photobio. B. **104**: 236-257, 2011.

Strasser, R.J., Tsimilli-Michael, M., Srivastava, A.: Analysis of the chlorophyll *a* fluorescence transient. − In: Papageorgiou GC, Govindjee (ed.): Chlorophyll *a* Fluorescence. A Signature of Photosynthesis. Pp. 321-362. Springer, Dordrecht 2004.

Tsimilli-Michael, M., Strasser, R.J.: In vivo assessment of stress impact on plants' vitality : applications in detecting and evaluating the beneficial role of mycorrhization on host plants. − In: Varma, A, (ed.): Mycorrhiza. Pp. 679-703. Springer, Berlin - Heidelberg 2008.

Yusuf, M.A., Kumar, D., Rajwanshi, R. *et al.*: Overexpression of gamma-tocopherol methyl transferase gene in transgenic *Brassica juncea* plants alleviates abiotic stress: physiological and chlorophyll *a* fluorescence measurements. – BBA-Bioenergetics **1797**: 1428-1438, 2010.

Zapata, J.M., Guéra, A., Esteban-Carrasco, A. *et al*.: Chloroplasts regulate leaf senescence: delayed senescence in transgenic *ndhF*-defective tobacco. − Cell Death Differ. **12**: 1277-1284, 2005.

Appendix

Fluorescence parameters in the kinetics of fast chlorophyll fluorescence rise and the formulae used for the calculation of biophysical parameters according to the JIP test.

F_0 ($\cong F_{20\mu s}$)	Minimal fluorescence intensity – when all RCs are open (considered as equal to the first credible measured intensity – at 20 μs).
F_m (= F_P)	Maximal fluorescence intensity – when all RCs are closed (due to the high actinic intensity used, it is considered that all RCs get closed at P).
F_v	Maximal variable fluorescence, $F_m - F_0$
F_J or F_I	Fluorescence intensity at 2 ms or 30 ms, respectively
V_K	$(F_{300\mu s} - F_0)/ (F_m - F_0)$, relative variable fluorescence at 300 μs
V_J	$(F_{2ms} - F_0)/ (F_m - F_0)$, relative variable fluorescence at 2 ms
V_I	$(F_{30ms} - F_0)/ (F_m - F_0)$, relative variable fluorescence at 30 ms
Flux ratios	
φ_{P0} or TR_0/ABS	$F_v/F_m = 1 - F_0/F_m$
ψ_{E0} or ET_0/TR_0	$1 - V_J = (F_m - F_J)/(F_m - F_0)$
δ_{R0}	$(1 - V_I)/(1 - V_J) = (F_m - F_I)/(F_m - F_J)$